Advanced techniques of laser telemetry

*SILVANO DONATI - **ALDO GILARDINI
*Electronics and Electrical Communication Institute - Pavia University **Research Department - Selenia

SUMMARY

After the examination of the constituted relationships which govern a laser telemeter, the noise sources and the accuracy of measurements obtainable with both pulsed and sinusoidal intensity modulation techniques are discussed. Various innovating developments in telemetry are then considered from the aspect of the instrumention philosophy and of optical detection.

1. Introduction

The instrumentation using laser sources to measure distances on the earth's surface can be classified under three headings, according to the applications and the use of the measurements.

1) Metrological interferometers (e.g. HP5525, Metrilas, etc. used in the mechanical industry, mostly for the calibration of machine tools) [1-3].
2) Geodimeters or topographical telemeters (e.g. HP, AGA, Eumig, etc. for the measurement of distances up to some hundreds of metres with precisions of about 1 cm) [4-6].
3) Military telemeters (for the measurement of distances up to about ten kilometres with precisions of some metres) [7-8].

In interferometers, use is made of a double optical path (measure and reference) for the propagation of two beams obtained by division of the beam emitted from the laser; the measurement path is that associated with a retroreflector mounted on the object of which the distance is desired. The recombination on the photo-detector after the propagation provides the so called interferometric measurement signal, or fringe signal of the type sin $(2\pi/\lambda)(L - L_r)$, which carries the information on the difference of the optical path $L\text{-}L_r$ as a fraction of λ, the wavelength corresponding to the phase velocity of the light. It should be noted that the detection process, due to the presence of the reference field, is coherent. In other terms, letting V_r, V as the amplitudes of the reference and signal fields, proportional to the root of the respective radiant powers, the electrical signal supplied by the photodetector is of the type $V_r V \sin (2\pi/\lambda)(L - L_r)$, i.e. it is attenuated as the root of the received power; in this sense the detection process is an optical homodyne.

In addition, if the two frequencies of the beams, on the reference and measurement paths, differ by a relatively small quantity $f_d = f_r - f$ (in the field of electrical frequencies, i.e. < 10 GHz) the process would actually be an optical heterodyne and in the sinusoidal term of the photo -detected signal a carrier $2\pi f_d t$ would appear.

We note also that the process of detection of the interferometer carries along a measurement philosophy: the sinusoidal term allows the counting of the fringe signals spaced by λ, and therefore by moving the retro-reflector along the measurement path we get its distance in units of λ (or fraction of it). The requirement of the interferometric method is obviously to have an adequately coherent source i.e. such that it will not introduce phase errors (in the sinusoidal term) between the fields recombined with different propagation delays; the He-Ne laser, which is easily stabilized in frequency [9], is an adequate source for this purpose.

Considering now the categories under headings 2) and 3) we find a quite different method of detection and measurement philosophy. The detection has been direct up to now, i.e. the output signal from the photodiode is of the type V^2 and it is attenuated as the received optical power; the distance information is extracted, as in common microwave radars, by imposing a sort of intensity modulation on the transmitted beam.

In the geodimeters the modulation is sinusoidal, as this waveform is highly suitable for the essentially continuous optical sources of modest power (e.g. LED's) used in these instruments. In the telemeters, however, the modulation is pulsed as it is easily obtained by using a laser in Q - switching regime (Nd and CO_2).

The instrumentation philosophies which directly derive from here are: a phase measurement between the received and transmitted signals in the sinusoidal modulation instrument, with the further refinement of introducing a frequency scanning or some similar provision to remove the ambiguity of distance (see below) and a time interval measurement in the pulse modulation telemeter, which takes advantage of the well developed techniques of wave-

form analysis suitable for the discrimination of diffuse and multiple echoes derived from radar and nuclear electronics.

It should be noted that in these cases we pass from phase and time data to that of distance through the group velocity of the source light. In this paper we assume that this velocity is equal to c, that of light in vacuum. In those cases where a better precision is necessary, the exact value of the group velocity must be considered; if this is not known, but the law of dependance of this velocity on the wavelength, it is possible to obtain the distance with a higher precision by effecting the measurements at several wavelengths.

As it will appear later, the instruments 2) and 3) based on direct detection, give a performance far from the quantum noise limit associated with the received signal, which is achieved on the other hand by the homo/heterodyne detection; generally they are limited by the noise of the photo-detector or of the background, which imposes a level depending on the performance of the receivers and on operating conditions, on the power of the source. The two types of modulation are shown to be equivalent regarding obtainable accuracy for the same energy available in the measurement time. Nevertheless, other accessory performances such as the discrimination of echoes and immunity to natural radiation favour the pulse approach because the duration of the signal is less and allows rejection of spurious waveforms.

In practice the availability of sources with sufficient peak power has up to now made not so important the optimum detection and measurement process from the point of view of the available energy; at present however this position is being reexamined and interesting research contributions have been made in this direction.

Below, after introducing the fundamental relationships regarding detection and measurement accuracy some new approaches that appear promising for some applications of second generation laser telemetry are discussed.

2. Propagation, attenuation and signal/noise ratio

The power attenuation in a telemeter, which usually operates on non cooperative targets or on diffusive surfaces, and that in a geodimeter, which operates with a cooperative retro-reflector (or corner cube) can be analysed with reference to Fig. 1. In view of the general nature of this article, which only claims to present overall evaluations, we neglect in all cases the losses due to the transmitting and receiving optics; it is however easy to introduce them in the calculations in practical cases.

Fig. 1

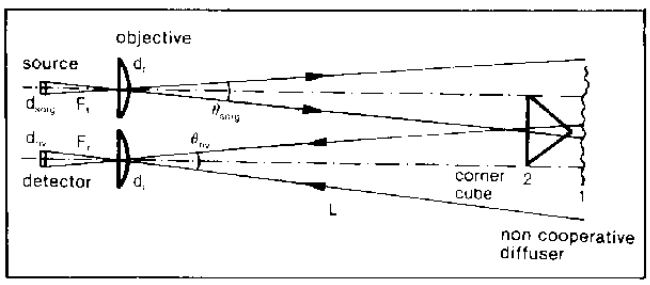

In the case of a non cooperative target, the transmitted spot has a diameter $L\ \vartheta_{sorg}$ at distance L, where $\vartheta_{sorg} = d_{sorg}/F_t$ is the divergence of the transmitted beam. If the dimensions of the target are greater than those of the spot, the entire transmitted power P_t is rediffused in accordance with the law of Lambert, in case with a diffusion coefficient $\delta < 1$ for grey surfaces, giving a light intensity in the orthogonal direction equal to $\delta\ P_t/\pi$. The receiver, which seen at the distance L presents a solid angle $\Omega_r = \pi d_r^2/4L^2$ thus receives a power P_r given by $(\delta\ P_t/\pi)\ \Omega_r$ and therefore:

$$\frac{P_r}{P_t} = \frac{\delta}{\pi}\,\Omega_r = \delta\,\frac{d_r^2}{4\,L^2} \tag{1}$$

on the assumption that the field of view of the detector, $\vartheta_{riv} = d_{riv}/F_r$, is greater than that of transmission, as is encountered in practice. If the diffusing area of the target (σ) is less than that of the spot ($\pi\ \vartheta^2_{sorg}\ L^2/4$), the ratio P_r/P_t is reduced in the ratio of the two areas i.e.:

$$\frac{P_r}{P_t} = \delta\frac{d_r^2}{4\,L^2}\,\frac{4\,\sigma}{\pi\ \vartheta^2_{sorg}\ L^2} = \delta\,\frac{\sigma\ d_r^2}{\pi\ \vartheta^2_{sorg}\ L^4} \tag{2}$$

where, as in microwave radars, the inverse dependance on L^4 appears. If for simplicity of notation the equivalent diameter of the target d_b is introduced according to the relationship $\sigma = \pi\ d_b^2/4$ the preceding relationship becomes:

$$\frac{P_r}{P_t} = \delta\,\frac{d_b^2\ d_r^2}{4\ \vartheta^2_{sorg}\ L^4}\ \left(\text{for}\ \frac{d_b}{L} \leq \vartheta_{sorg}\right) \tag{3}$$

It may also be pointed out that in the texts dealing with laser telemeters often the solid angle of the transmitted beam Ω_T ($\simeq \vartheta_T^2$, ϑ_T being the beam width according to the normal definition used in the theory of antennas) is used instead of ϑ_{sorg}. The area of the spot is then $\Omega_T L^2$, from which $\Omega_T = \pi\ \vartheta^2_{sorg}/4$.

In the case of a co-operative reflector, since this forms an image of the source at double the distance from it, the attenuation is readily given by:

$$\frac{P_r}{P_t} = \frac{\text{receiver area}}{\text{spot area at dist. } 2L} = \frac{d_r^2}{4\ \vartheta^2_{sorg}\ L^2} \tag{4}$$

under the condition that the size of the corner cube does not reduce that of the spot seen at the receiver. Comparing eqns (1) and (4) it is seen that the retro reflector permits a gain equal to $1/\vartheta^2_{sorg}$ in the received power with respect to the ideal diffuser, and this explains the disparity of values necessary for the powers in the two cases.

A further contribution to attenuation, beyond the geometrical comes from the absorption and diffusion of the propagation medium. Since the attenuation follows Beer's law, for a path length 2L we have:

$$P = P_0 \exp\,(-\,2\,\alpha\,L) = T^2_{atm}\,P_0 \tag{5}$$

where $\alpha = \alpha\,(\lambda)$ is the coefficient of attenuation, depending on the wavelength employed and on the meteorologi-

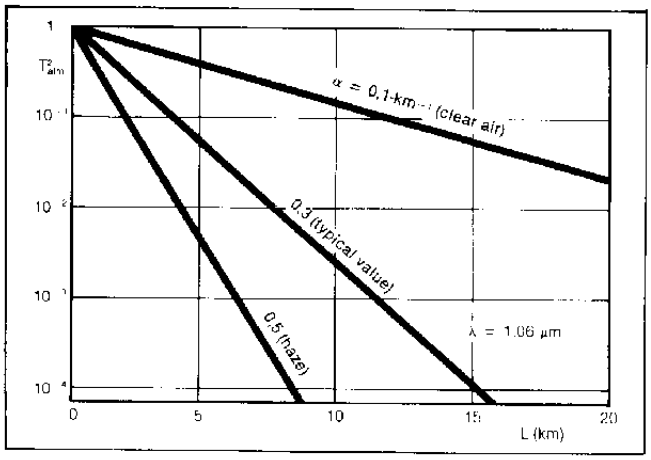

Fig. 2

cal conditions, and which is usually between 0.1 and 0.5 km^{-1} at λ = 1.06 μm [10-11] (see Fig. 2).

It should be noted that atmospheric attenuation T^2_{atm}, to be inserted formally in the second member of eqns (1-4), while it is in practice negligible up to L = 1 km, can become very high for the maximum operating distances of a telemeter.

In relation to the wavelength, the behaviour of the solar spectrum to the diverse air masses (AM) shown in Fig. 3 [12] is indicative of the windows of maximum transparency in the near infra-red, or of the corresponding laser sources suitable for telemetry.

Once given the attenuation P_r/P_t from equations (1-4) and a value $(S/N)_i = P_r/P_n$ for the input signal/noise ratio, the requirement of transmitted power P_t is expressed as:

$$\frac{P_t}{P_n} = \frac{4\,L^2}{G\,d_r^2\,T^2_{atm}}\,(S/N)_i \qquad (6)$$

where: $G = 1/\vartheta^2_{sorg}$ for cooperative targets (topograph)
$= \delta$ for diffusive targets (telemeters)
$= \delta\,(d_h/\vartheta_{sorg}\,L)^2$ for diffusive targets when $d_h/L < \vartheta_{sorg}$.

Fixing reasonable values for the signal-to-noise ratio (S/N = 10) and for the diameter of the receiving optics (d_r = 100 mm) we obtain the universal diagram of Fig. 4 for the transmitted equivalent power GP_t against the normalized distance L/T_{atm} and with the noise power (NEP) P_n as a parameter.

Fig. 4 shows the regions corresponding to typical

Fig. 3

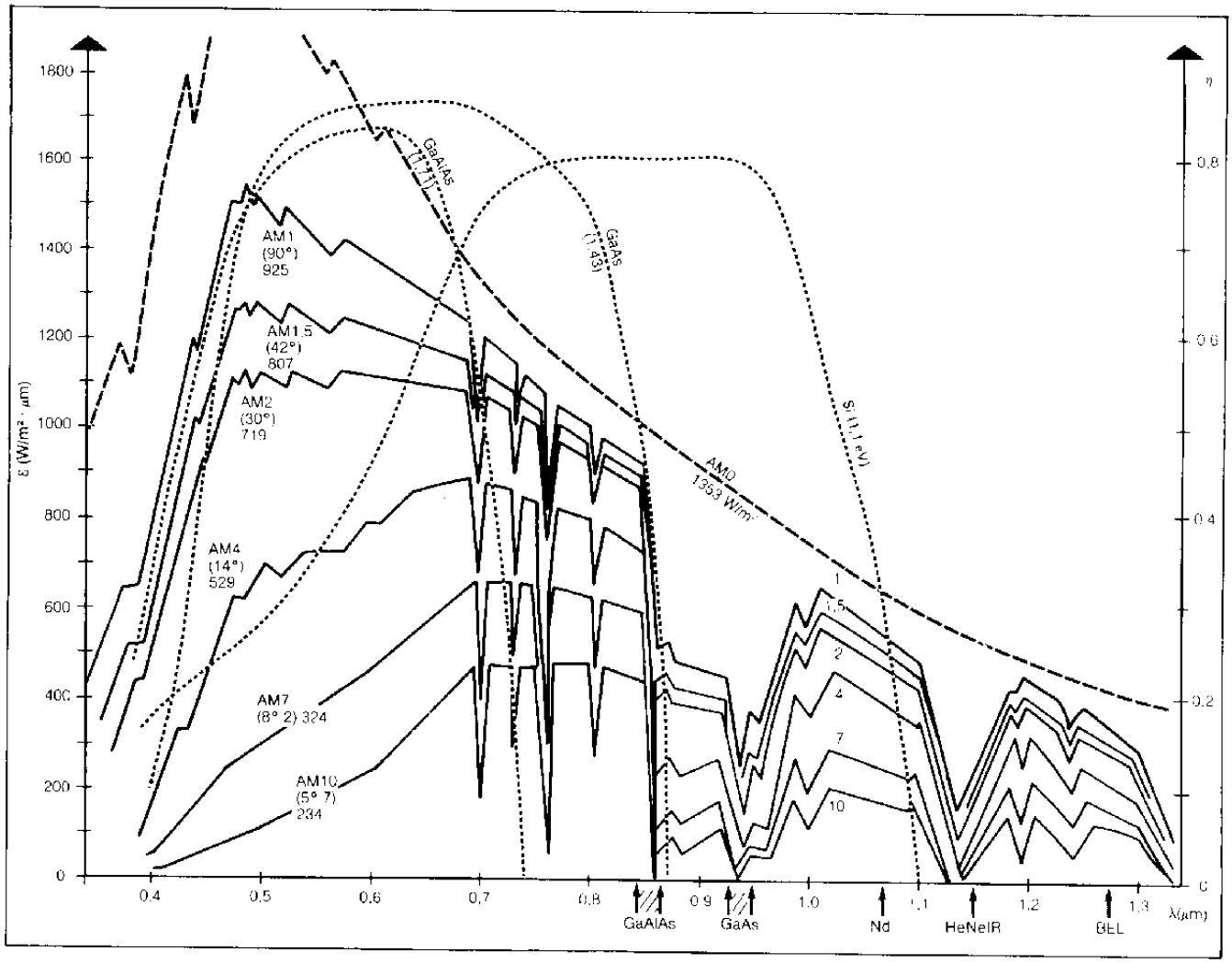

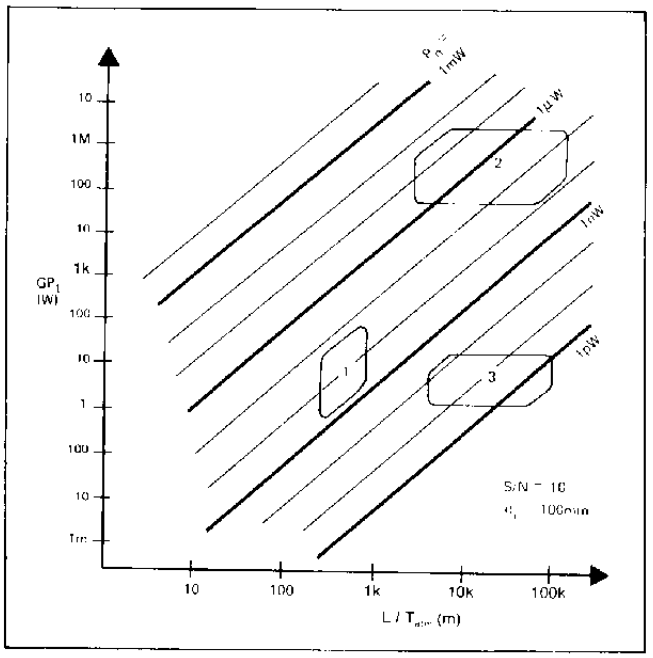

Fig. 4

present-day topographs [1] which operate with G = 10^3 -10^4 and powers of the order of a milliwatt, of conventional Nd pulsed telemeters [2] which operate with G = 0.03 - 0.3 and powers from 1 to 10 MW and of a hypothetic continuous wave telemeter [3] with sinusoidal modulation and powers of the order of watts.

2.1 NOISE EVALUATION

It is important to determine the relative weight of the various noise sources which contribute to give P_n. Further, the evaluation of P_n for a specific telemeter, by use of the diagram in Fig. 4, allows us to determine if the performances at distance L are achieved with the employed power GP_t; knowing P_n we may then calculate also the measurement errors.

It should be remembered first of all that the current at the output of the photodetector i_r is proportional to the optical power P_r according to the expression:

$$i_r = \frac{M \eta e}{h \nu} P_r \qquad (7)$$

where η is the quantum efficiency of the detector and M is the multiplication factor of electrons in the detector (> 1 for photomultipliers and avalanche diodes, = 1 for the other photodetectors without gain). The factor ($M \eta e/h \nu$) in A/W is the sensitivity or responsivity of the photodetector.

The fundamental noise contributions, which we shall express in terms of equivalent optical noise power at the input of the detector (which is defined as NEP), are as follows:

a) The quantum (or shot) noise associated with the detector signal P_r, which is:

$$P_{rn} = \left[\frac{2 h \nu}{\eta} F(M) P_r B \right]^{1/2} \qquad (8)$$

where B is the measurement bandwidth and F (M) is a factor that represents the excess noise due to the multiplication M. This is obviously the intrinsic limit below which the overall noise cannot fall.

b) The shot noise associated with the background illumination P_f seen from the area to which the detector is pointed, which is:

$$P_{fn} = \left[\frac{2 h \nu}{\eta} F(M) P_f B \right]^{1/2} \qquad (9)$$

where the background power P_f collected by an optics with an aperture number NA, detector diameter d_{riv}, which is pointed on a scene having spectral irradiation ϵ (W/m^2 μm) and diffusion δ is given by:

$$P_f = \epsilon \delta \Delta\lambda (\pi d_{riv}^2 / 4) NA^2 \qquad (10)$$

and $\Delta\lambda$ is the bandwidth of the filter placed before the detector (or the equivalent width of the spectral response of the detector itself). This contribution is especially important for low received power, or for continuous wave operation, where it may be the dominant term which one tries to reduce with a narrow band $\Delta\lambda$ interference filter.

c) The electronic noise of the receiver, given by:

$$P_e = \frac{h \nu}{M \eta e} \left[\frac{4kT}{R_{eq}} B \right]^{1/2} \qquad (11)$$

where R_{eq} is the noise equivalent resistance of the receiver at the input of the preamplifier. In general, while at moderate bandwidths (of the order of kHz's) the equivalent resistance can be made very high because the termination does not reduce the frequency performance, with the increasing of the bandwidth the R_{eq} obtainable with a good circuit design strongly diminishes.
For example we may have R_{eq} = 10-100 M Ω at B = 1 kHz but only R_{eq} = 5-10 kΩ at B = 50MHz. This circumstance favours the continuous wave telemeters with respect to the pulsed ones.

d) The noise for the dark current, given by:

$$P_b = \frac{h \nu}{M \eta e} (2 e B)^{1/2} (i_s + M^2 F(M) i_v)^{1/2} \qquad (12)$$

where i_s is the term without gain (of surface in photodiodes) of the dark current and $i_v \ll i_s$ is the term with gain (of volume in photodiodes) of this current.

By summing the squared contributions of noise, since they are uncorrelated, we obtain for the total noise P_n:

$$P_n^2 = \frac{2 h \nu}{\eta} F(M) (P_r + P_f) B + \left(\frac{h \nu}{M \eta e} \right)^2 \cdot$$

$$\cdot \left(2 e i_s + 2 e M^2 F(M) i_v + \frac{4kT}{R_{eq}} \right) B$$

$$= \frac{2\,h\,\nu}{\eta}\left[F(M)\left(P_r + P_f + \frac{h\,\nu}{\eta\,e}\,i_v \right) + \right.$$

$$\left. + \frac{h\,\nu}{M^2 \eta\, c}\left(i_s + \frac{2kT}{e\,R_{eq}} \right) \right] B$$

$$= \frac{2\,h\,\nu}{\eta}\left[F(M)\,(P_r + P_f + P_v) + \frac{P_{eq}}{M^2} \right] B \qquad (13)$$

heaving let:

$$P_v = \frac{h\,\nu}{\eta\,e}\,i_v \qquad (13')$$

$$P_{eq} = \frac{h\,\nu}{\eta\,e}\left(i_s + \frac{2kT}{e\,R_{eq}} \right) \qquad (13'')$$

P_{eq} has the meaning of an equivalent optical power for the noise due to the dark current and to the electronics of the receiver, P_v an equivalent optical power for the component i_v of the dark current.
In the limit case P_f, P_v, $P_{eq} \ll P_r$ we have the maximum value of the $(S/N)_i$ ratio, i.e.:

$$\left(\frac{S}{N} \right)_i = \frac{P_r}{P_n} = \left[\frac{\eta\,P_r}{2\,h\,\nu\,F(M)\,B} \right]^{1/2} \qquad (14)$$

which represents the quantum noise limit of this ratio.

Fig. 5 shows separately, according to the corresponding power levels, the values of the three quantum, background and electronic noise contributions, (the contributions due to dark current will not be considered now, but will be discussed later) for two hypothetical cases of telemetry at a wavelength of 1.06 μm (corresponding to Nd lasers) with B = 10MHz and P_t = 3 MW (for pulsed operation) and with B = 10Hz, P_t = 3W (for continuous wave).

It is assumed furtherly a distance L = 1 Km, an optics with d_r = 100 mm, a photo detector without gain (M = 1) but with unity quantum efficiency, equivalent resistances of 10 k Ω and 10 M Ω respectively and δ = 0.3, T^2_{atm} = 0.1; for the background spectral radiation ϵ the value is assumed at λ = 1.06 μm given from Fig. 3 with AM 1.5 (from Ref [10]) and also in eqn (10): d_{ov} = 0.25 mm and NA = 0.5; it is finally assumed that $\Delta\lambda$ = 10 nm for the CW telemeter alone (for the pulsed one P_f is already less than P_{eq}, P_r without filters).

As we can see in Fig. 5, there is a difference of four orders of magnitude betwen the noise in the two cases, and while for the pulse telemeter we have $P_r > P_{eq}$, for the CW one the performance is dominated by P_f, $P_{eq} \gg P_r$.

These results are valid for L = 1 km, while if we pass to L = 10 km, P_r decreases by more than two orders of magnitude, and therefore also for the pulsed telemeter P_r becomes less than P_f and P_{eq}. Thus at maximum range, a telemeter with direct detection operates in conditions which are not optimum, since it does not reach the quantum limit (14).

In the preceding calculations of P_{eq} the dark current i_s has not been considered; on the basis of eqn (12) this current should be added to the electronic term $(2kT/e\,R_{eq})$ which, with the values of R_{eq} assumed above, is equal to 5

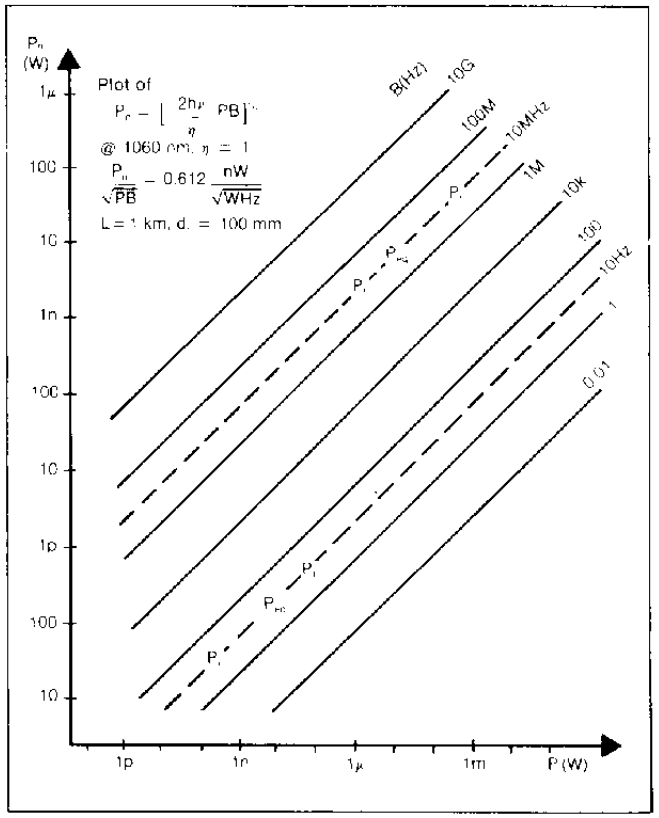

Fig. 5

μA for the pulsed telemeter and 5 nA for the CW one. The dark current i_s in the photodiodes without multiplication reaches at maximum some tens of nanoamperes; this means that the term due to the dark current is negligible in the case of the pulsed telemeter, while in the case of the CW one photodiodes with sufficiently low dark currents are chosen (of the order of nanoamps) in order to not significantly worsen the performance.

If photodetectors with multiplication are employed, e.g. an avalanche photodiode with M = 50 to 100 and F (M) = 2-3, the contribution of the electronic noise P_{eq} to the total noise decreases as determined in equation (13) so that, at the limits of the range of the telemeters considered, the dominant noise is the shot noise associated with the background P_f or that due to the volume component of the dark current P_v.

The probabilities of detection and false alarm in a laser telemeter depend on the statistical characteristics of the noise, about which we have not spoken up to now, limiting ourselves to consider the average power.

If the number of received photons is small, it is necessary to know with precision the statistics of the relative photoelectrons, but if the number is great, by the central limit theorem it may be assumed that the distribution of these photoelectrons is sufficiently well represented by the gaussian distribution.

Since we have seen that often in the cases considered the dominant noise is that associated with the background, we calculate how many photoelectrons are generated on average by the background P_f in the observation time τ = K/B, where K is of the order of unity (typically 0.5); this number will be:

$$N_f = \frac{\eta\,K\,P_f}{h\,\nu\,B} \qquad (15)$$

It is immediately verified that in the case of a pulsed telemeter there is a smaller number of photoelectrons, but also in this case a number in the order of a million is obtained, and therefore such as to justify the assumption of a gaussian distribution.

In this case many results already known from the theory of microwave radars [7] [13] are applicable, and in particular for a given probability of detection and for a given probability of false alarm the required S/N ratio may be determined. Further, if the detection is performed after the integration of several pulses, the results which in the theory of microwave radars are used for the case of integration after detection may altogether be utilized.

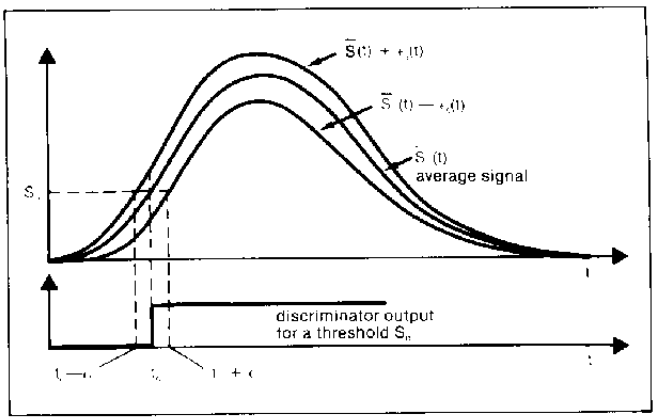

Fig. 6

3. Analysis of the accuracy of pulse and sinusoidally modulated telemeters

We will now examine the accuracy of direct detection telemeters with different intensity modulations, i.e. pulsed or sinusoidal, to establish its dependence on the equivalent noise power P_n just seen and on the measurement time. The result of the analysis is that, analogously to the case of the microwave radars, there is an essential dependance not on the received signal bandwidth, but on the product of the measurement time and the received power, i.e.on the energy, at least as theoretically obtainable performance if other causes of systematic error (which in principle may be eliminated) do not occur.

3.1 ACCURACY OF THE PULSED TELEMETER

The measurement of distance L is performed as a measurement of the time of flight i.e. of the time interval between two electrical pulses, the reference one obtained with the generation of the transmitted pulse and the measurement one which is that received after propagation at the photodetector.

Since the reference can be taken with an amplitude as large as desired, let us neglect the time error associated with the amplitude discrimination of it, which gives the zero-time of the measurement. The received pulse S (t), however, can be represented (fig. 6), as the sum of an average component $\bar{S}$ (t) and of a fluctuation with r.m.s. value ϵ_s (t). If ϵ_s (t) $\ll \bar{S}$ (t), i.e. the process is a linear regression around a threshold S_o, which represents the switching level of a discriminator handling the detected signal, the time error ϵ_t is simply given by (fig. 6):

$$\text{(time error)} = \frac{\text{(amplitude error)}}{\text{(average slope)}}, \text{ i.e } \epsilon_t = \frac{\epsilon_s(t)}{\left[d\,\bar{S}(t) \mid dt \right]} \tag{16}$$

In terms of the received peak power P_r and of the normalized waveform s (t/τ), we may write:

$$\bar{S}(t) = P_r\, s\,(t/\tau),$$

$$\frac{d}{dt}\bar{S}(t) = P_r \frac{1}{\tau} s'(t/\tau) \tag{17}$$

where for s (t/τ) the following properties are valid: max s $(t/\tau) = 1$; $\int_0^\infty s\,(t/\tau)\,dt = \tau$ (which defines the duration τ of the pulse). Inserting eqn (17) in eqn (16) and calculating ϵ_s with eqn (13), in which we put $B = K/\tau$ and incorporating P_v in the term P_f, we have:

$$\epsilon_t = \tau^{1/2} \frac{(2\,K\,h\nu/\eta)^{1/2}\,[F\,P_r\,s\,(t/\tau) + F\,P_f + P_{eq}/M^2]^{1/2}}{P_r\,s'(t/\tau)} \tag{18}$$

which is of the type:

$$\epsilon_t = \tau \left(\frac{A'}{E_r} + \frac{A''}{E_r^2} \right)^{1/2} \tag{19}$$

where $E = P\,\tau$ is the energy content in a pulse of power P and width τ and:

$$A' = \frac{2\,K\,h\nu\,F\,s\,(t/\tau)}{\eta} \frac{}{s'(t/\tau)^2} \tag{20}$$

$$A'' = \frac{2\,K\,h\nu\,FP_f + P_{eq}/M^2}{\eta} \frac{}{s'(t/\tau)^2}\,\tau = \frac{2\,K\,h\nu\,FE_f + E_{eq}/M^2}{\eta} \frac{}{s'(t/\tau)^2}$$

In a pulsed telemeter, as long as the peak signal P_r is of sufficiently large power to dominate with its own quantum noise the other background and electronic contributions, as for example in the case of Fig. 5 ($P_r > P_{eq}, P_f$), a situation which is obviously valid for the short distances up to a certain L_o, we have:

$$\epsilon_t \simeq \tau\,(A'/E_r)^{1/2} \qquad (L < L_o) \tag{21}$$

i.e. the measurement error of the time ϵ_t is proportional to the duration τ of the pulse and inversely to the root of the total energy E_r available during the measurement time τ.

Note also that eqn (21) can be written in the form:

$$\epsilon_t \simeq F_s \frac{\tau}{\sqrt{N_r}} \tag{22}$$

where $N_r = \eta E_r/h\nu$ is the number of photons detected per pulse, and $F_s = (2 KF\ s/s'^2)^{1/2}$ is a numerical factor of the order of unity, which depends on the position of the threshold level S_o (Fig. 6) though the term s/s'^2.

In the operation at great distances, $L > L_o$, when the signal P_r is very weak, the noise terms P_{eq}, P_f predominate, and for the time error we have:

$$\epsilon_t \simeq \tau \sqrt{A''}/E_r \qquad (23)$$

and now dependence is of inverse proportionality to the detected energy (or to the number of photons $\eta E_r/h\nu$). Taking into account eqns (1) and (4) and the relationship $\epsilon_L = c\,\epsilon_t/2$ between the errors of distance and time, and neglecting the effect due to the attenuation of the propagation medium, we obtain the schematic diagram of Fig. 7, which shows how the relative error is constant as long as the quantum noise predominates, i.e. up to a certain distance L_o, while it increases as the distance L for $L > L_o$ where the electronic and background noise predominate.

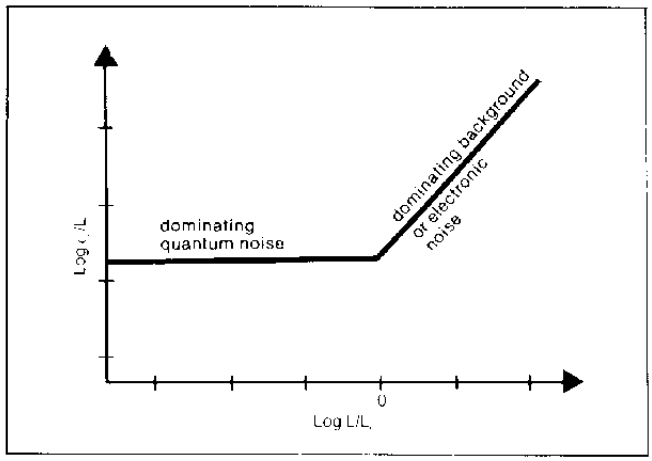

Fig. 7

3.2 OPTIMUM FILTER FOR TIME LOCALIZATION

The time accuracy ϵ_t, in a threshold S_o crossing circuit, which we have up to now considered as the method of measurement, depends through the factor A' of eqn (20) on the ratio s/s'^2 between signal amplitude and slope, indicating how it will then be necessary to position the threshold where the squared slope is maximum respect to the amplitude to obtain the best ϵ_t. It should be noted however that a time measurement by threshold crossing, even if this is positioned at an optimum level S_o, nevertheless is not optimum as far as the extraction of all the information associated with the waveform is concerned. The latter also contains, at levels different from S_o, some more information on time localization.

Let us now consider the block diagram in Fig. 8 where a filter with a pulse response h (t) which, for a certain signal waveform S(t), minimizes the time error ϵ_t, is placed in cascade with the photodetector PD. In effect at the output of the optimum filter the signal has in general an amplitude S_u (t):

$$S_u(t) = \int_0^\infty S(y)\, h(t - y)\, dy \qquad (24)$$

and an amplitude variance:

$$\epsilon_{su}^2(t) = \int_0^\infty \epsilon_s^2(y)\, h^2(t - y)\, dy \qquad (25)$$

from which, by inserting these expressions in eqn (16) and minimizing ϵ_t with respect to the class of the functions h (t) (with a variational method of Hilbert) we find the pulse response of the optimum filter [14]:

$$h(t) = \frac{S'(T_m - t)}{S(T_m - t) + \rho} \qquad (26)$$

where:

$$\rho = [P_f + P_{eq}/M^2 F(M)] / P_r = [E_f + E_{eq}/M^2 F(M)] / E_r \qquad (27)$$

and a corresponding optimum value of ϵ_t at the measurement time T_m:

$$\epsilon_t = \tau \left[\frac{2 K h\nu}{\eta} \frac{F}{E_r} \Big/ \int_0^\infty \frac{s'(t/\tau)^2}{s(t/\tau) + \rho}\, d(t/\tau) \right]^{1/2} \qquad (28)$$

When $L > L_o$, i.e. at large distances, $\rho \gg 1 > s(t/\tau)$ and the optimum filter is that with pulse response $h(t) \propto S'(T_m - t)$ i.e. coincides with the optimum filter normally considered in the receivers of microwave radars [13]. At short distances for which $L < L_o$, ρ may however be ignored; it results that the optimum filter in that case is:

$$h(t) = S'(T_m - t) / S(T_m - t) \qquad (29)$$

This case deserves further discussion both because it differs from what is known for microwave radars and because it is precisely at short distances that the accuracy becomes more important in the use of a telemeter.

Comparing with the equations (20) (21) we see that the obtainable improvement lies within the term cointaining the signal waveform, which passes to $\int_o^\infty [s'(t/\tau)^2 / s(t/\tau)]\, d(t/\tau)$ from the value $s'(t/\tau)^2 / s(t/\tau)$.

The ratio of these quantities, which represents the obtainable reduction of the variance, obviously depends on

Fig. 8

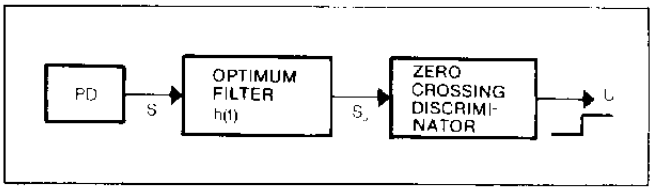

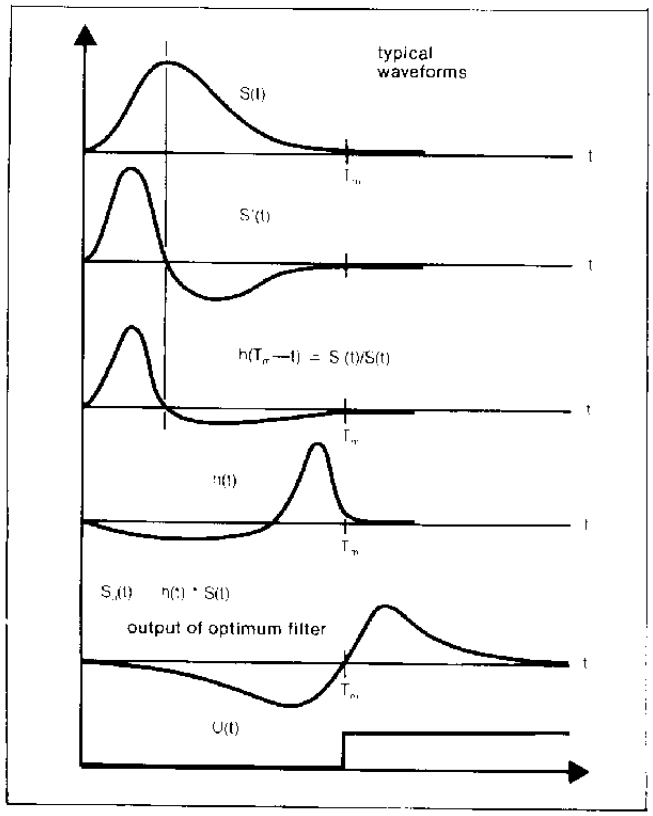

Fig. 9

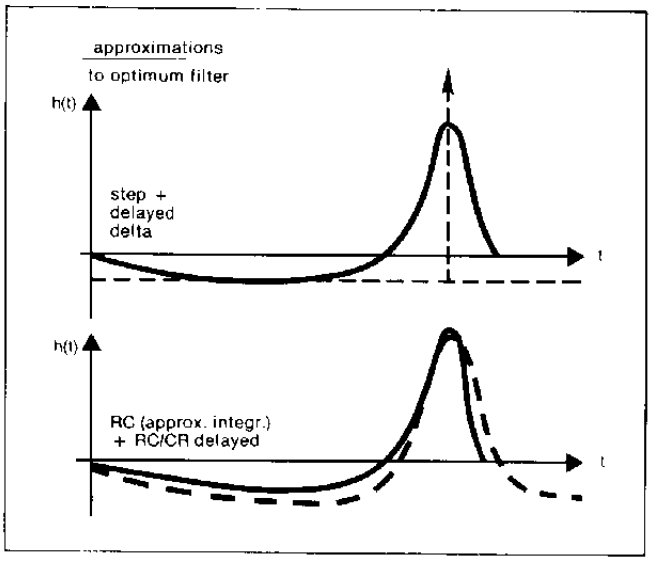

Fig. 10

the type of waveform and is within the range of typical values 1-5. In special cases, it is found that the optimum filter becomes a delta for step waveforms (with very steep rising edges) and is a ramp for a gaussian waveform. Fig. 9 shows the waveforms for optimum filtering for a response of the (29) type in the various points of the block diagram of Fig. 8.

As shown in Fig. 9, and the result is quite general, the output of the optimum filter passes through zero at the measurement instant T_m. So this is easily determinable with a zero crossing discriminator, as shown in Fig. 8.

We will now look briefly at the problem of the synthesis of the optimum filter for a response such as that of Fig. 9, which is a problem of approximation in the time domain of a pulse response.

Usually, if the improvement of the optimum filter comes from the elimination of fluctuations of the amplitude of the pulse S(t) only (and not of its shape), a step plus a delayed δ (t) is a good approximation [14] (See Fig. 10).

The conformity to the optimum response can be improved if we sharpen the preceding filter as an approximate integrator plus a delayed approximated differentiator, then properly adjusting the time constants RC which govern the two cells of this combination.

In general, with this method we can already approach close to the optimum performance within for example 10% [15]. On the other hand, for waveforms S(t), which are significantly different from the typical ones of Fig. 9, an approach of synthesis of the pulse response by means of transversal filters, e.g. realized with CCD and BBD elements, may be preferable.

3.3 ACCURACY OF THE SINEWAVE TELEMETER.

For continuous sources, the sinusoidal modulation of the intensity is an adequate method for the high precision measurement of flight time [16] [17].

Let us suppose then that the trasmitted signal is of type P (1 + cos 2 πf t) so that the measurement of distance will be made by measuring the phase shift between the received signal:

$$P_{ric} = P_r [1 + \cos 2\pi f (t - 2 L/c)] \qquad (30)$$

and the reference one:

$$P_{rif} = P_0 [1 + \cos (2 \pi ft - \varphi_0)] \qquad (31)$$

The phase signal is contained in the beating waveform $< P_{ric} P_{rif} >$ at the output of a mixer circuit:

$$S = P_r P_0 \cos \left(2 \pi f \frac{2L}{c} - \varphi_0 \right) \qquad (32)$$

This signal can be averaged for the whole measurement time, which we will call T_r (from which we obtain a measurement bandwidth B = K/T_r, with K = 0.5). Around the reference phase-shift value $\varphi_0 = 2\pi f (2L/c) + \pi/2$, the point of maximum sensitivity, obtainable in general for any distance L by introducing a variable electronic delay of the reference, the phase error is:

$$\epsilon_\varphi = P_n / P_r \qquad (33)$$

where P_n is given by eqn (13). To compare the result with eqn (19) valid for the pulse mode, we express the time error $\epsilon_t = \epsilon_\varphi / 2 \pi f$ with eqn (33), so obtaining:

$$\epsilon_t = \frac{1}{2\pi f}\left(\frac{2K h\nu}{\eta}\right)^{1/2} \cdot \left(\frac{F}{P_r T_r} + \frac{F P_f + P_{eq}/M^2}{P_f^2 T_r}\right)^{1/2} = \frac{1}{2\pi f}\left(\frac{B'}{E_r} + \frac{B''}{E_r^2}\right)^{1/2} \quad (34)$$

where:

$$B' = \frac{2K h\nu}{\eta} F$$

$$B'' = \frac{2K h\nu}{\eta} (FE_t + E_{eq}/M^2) \quad (35)$$

When the first term predominates, i.e. we work in conditions of quantum noise, the sinusoidal telemeter gives a performance substantially equivalent (apart from a numerical factor of the order of unity) in precision to the pulsed one, for equal energy $E_r = P_r T_r$ detected in the measurement time and for equal modulation time duration $\tau = 1/2\pi f$.

In practice, since P_r is now much less than the pulsed power, in the direct detection mode the second term almost always predominates.

We may also set eqn (34) in the form:

$$\epsilon_t = \frac{1}{2\pi f}\left(\frac{B'}{E_r}\right)^{1/2} (1+\rho)^{1/2} \quad (36)$$

where ρ, the multiplicative factor which gives the worsening with respect to the quantum performance, is given for direct detection by the expression (27), i.e. by the ratio between the equivalent background and electronic powers and the quantum noise power. It has to be noted how, in the sinusoidal modulation approach for telemetry, the high frequencies f which are necessary imply an ambiguity in measurement, since the phase shift $2\pi f (2L/c)$ is much greater than 2π and the phase is measured with modulus 2π

The ambiguity is removed with various provisions (see Para. 4.1. and 4.2) which, while implying the use of part of the measurement time T_r for the coarse distance measurement, can be performed in a fraction of this time (or with a fraction of the dedicated power P_r), without substantially worsening the precision of the fine measurement of which eqn (36) provides the value.

4. Instrumental developments for CW or long-pulse telemetry

4.1 FREQUENCY SCANNING TECHNIQUE OF CW TELEMETRY

To remove the ambiguity in the 2π modulus phase measurement, one of the first instrumental techniques adopted in the sinusoidal wave telemeters has been that of making a frequency scan, so as to be able to carry out an accurate measurement of φ with a high maximum frequency f_M, and have a large distance of ambiguity $L_a = c/2f_m$ (corresponding to φ which equals 2π) because of the small value of the minimum frequency f_m. Tacking, for example, $L_a = 15$ km we have $f_m = 10$ kHz as minimum frequency; and we will have on the other hand $f_M = 15$ MHz as the maximum frequency necessary for resolving $\Delta L = 10$ cm as one-hundredth of 2π rad.

The measurement technique consists in counting the zero crossings of the beat signal, each of which indicates that at that moment a whole number of half wavelength corresponding to the difference frequency between the instantaneous modulation frequency f_{is} and the minimum frequency f_m are contained in the measurement distance L. At the end of the sweep, since $f_M \gg f_m$, this number will then be the whole number of phase round angles we

Fig. 11

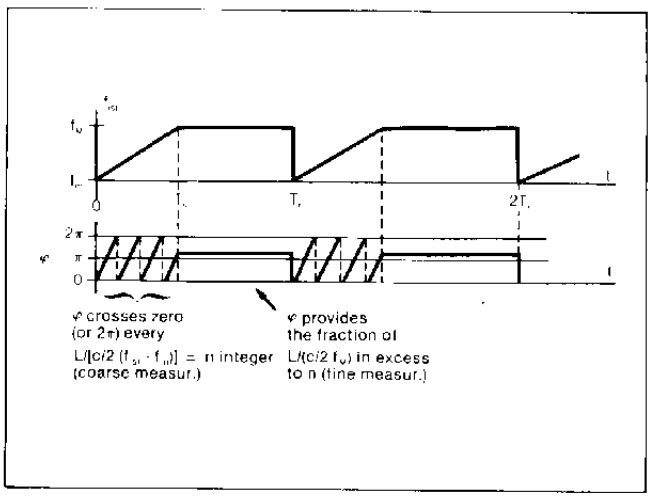

Fig. 12

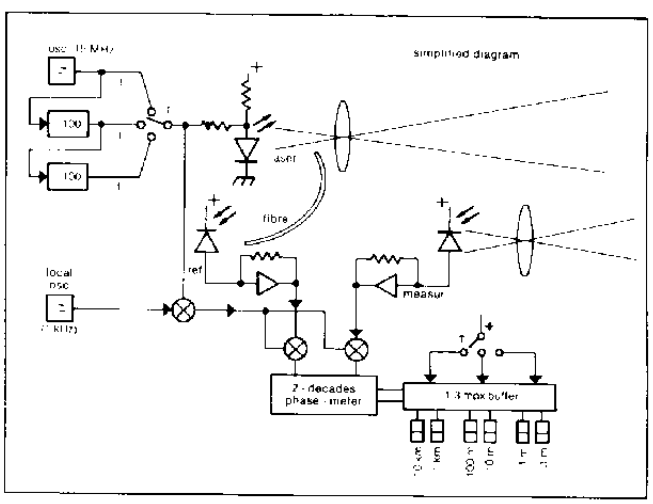

must add to φ, i.e. the number of intervals $c/2\ f_M$ (= 10 m in the example quoted above) to be added to the value $(\varphi / 2\ \pi)$. $c/2\ f_M$ (see Fig. 11).

Imposing to the source the frequency waveform of Fig. 11 by means of a generator which feeds a VCO, the output of which drives the laser source modulator, a control signal is extracted which serves to perform the coarse measurement in the time window O-T_s with a zero counter and the fine one in the time window T_s - T_r with a two-decade phase meter (resolution of 2 π/100). We may note that, to integrate the signal in the time O-T_s, i.e. to reduce the noise that especially in the zero crossings can give rise to counting errors, we may use a PLL with a locking time constant not much less than T_s and centred on the frequency $f_c = (f_M - f_m)$. $2L/cT_s$ supplied during the scanning at the output of the demodulator.

For example, for T_s = 100 ms, we have f_c = 15 kHz for L = 15 km, and the time T_r-T_s can be held comparable to T_s.

4.2 MULTIFREQUENCY TECHNIQUE FOR THE CW TELEMETER

Let us consider a geodimeter where three modulating frequencies are used in sequence yielding a distance resolution of six decades:

f_1 = 15 MHz (L_M = 10m)

f_2 = 150 kHz (L_M = 1 km)

f_3 = 1.5 kHz (L_M = 100 km)

For each frequency the phase $\varphi_i = 2\ \pi\ f_i(2L/c)$ is measured with resolution of two decades by means of a single phase meter which operates at an intermediate frequency of 1 kHz to which all the three beats are shifted, and the result is stored in the two decades of the corresponding range. The advantage of this solution is that for each frequency, in the presence of a radial velocity component of the object, the latter can be determined or corrected for.

Further, it is easier to balance the phase drifts in the electronics by using as a reference a part of the optical signal taken from the source by means of an optical fibre, as shown schematically in Fig. 12; even better is to use a single avalanche diode for reference and measurement, feeding it alternately with the two optical signals, by means of a mechanical chopper. Since the corresponding electrical signals are not then present simultaneously at the input of the phase meter, two PLL's which are connected alternately to the photodiode are used. It also be noted that to synchronize the bits of the less significant decades with those of the more significant ones, it is necessary that the phase measurements associated with f_2 and f_3 be discretized in intervals of 1/200 of the round angle (instead of 1/100) so as to be able to apply a Gray code method of synchronization for redundancy [18].

A typical multifrequency geodimeter is the Hewlett Packard HP 3850 A, where the source is a GaAs laser which delivers 60 μW and the receiver is an avalanche photodiode which operates within the range P_r = 20pW-60nW. The divergence of the source is ϑ_{sorg} = 1 mrad ($G = 10^6$) and the maximum range of the instrument is L = 8 km with retroreflector.

It may be noted that this technique, as the preceding one, is not immune from errors caused by retrodiffusion from the medium or from extended target echoes; on the signal is superimposed an interference, which is given by the sum of the contributions (phasors) coming from the single illuminated retrodiffusing elements and which is indistinguishable from the signal (unlike what occurs with pulsed telemetry).

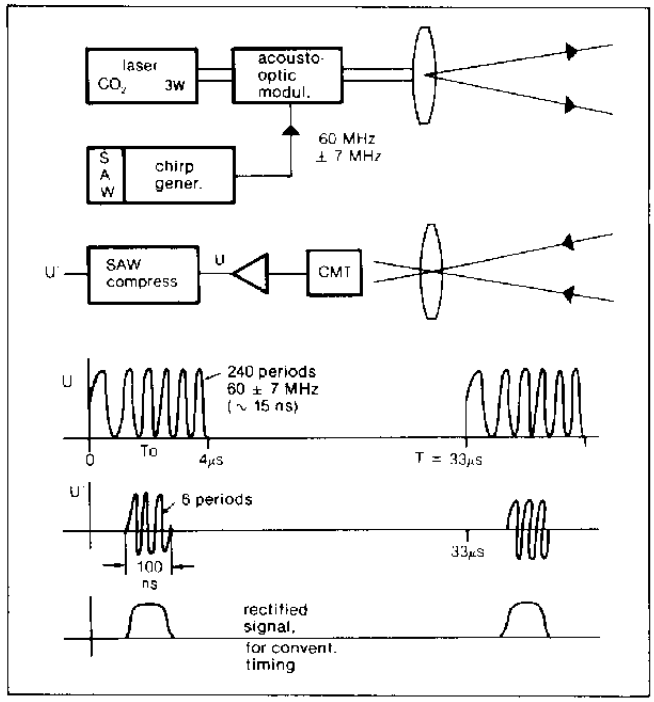

Fig. 13

4.3 PULSE COMPRESSION TECHNIQUE

This technique, already well known and used for microwave radars [13], consists in trasmitting a CW or pulsed-signal modulated by means of a waveform or a suitable code, and in cross-correlating the detected echo, which supposedly will not have lost the information contained in the modulation, with the waveform or code transmitted. At the output there is a compressed pulse of width approximately $1/B_m$ where B_m is the bandwidth of the modulated signal used. Therefore this solution guarantees, if B_m is sufficiently large, the obtaining of detection and accuracy performance in the measurement of distance which are truly those of the very short pulsed telemeters.

The application of this technique to telemetry has been especially studied in England at RSRE: the most important theoretical aspects for the optic case have been analysed and discussed by Oliver [19], while an experimental development has been recently presented by Hume and others [20].

These authors have chosen a chirp pulse for the instrumental realization, i.e. a pulse within which there is a sinusoidal oscillation whose frequency varies linearly in time.

The instrumental approach has been applied to a CO_2 laser, stabilized in frequency with a continuous output P_{CW} = 3W, but it is just as appropriate for near infrared sources with continuous emission or long pulses (widths of some microseconds). Further, in this case it is convenient and natural to employ heterodyne detection of the reflected signal; this however is an additional technique,

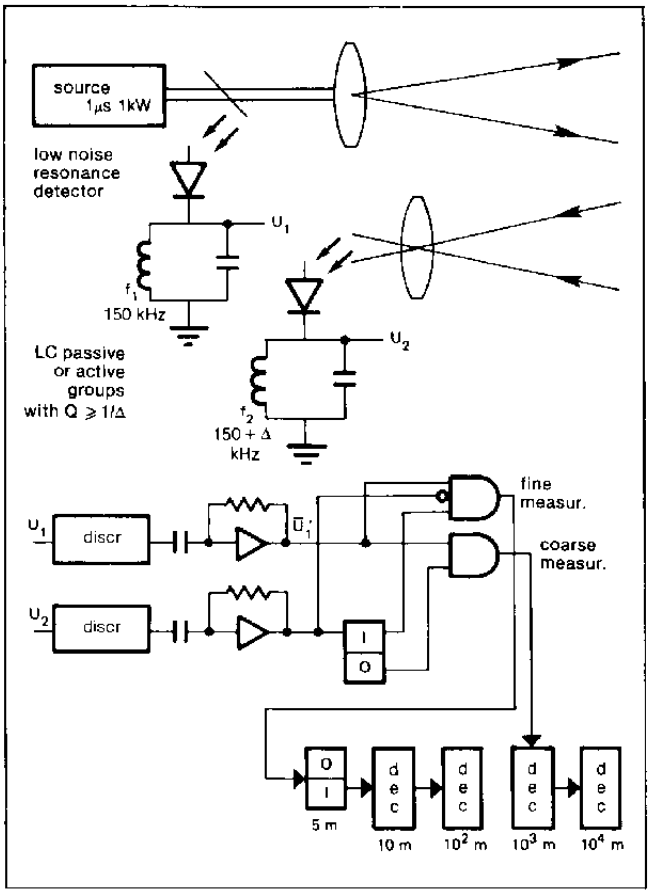

Fig. 14a

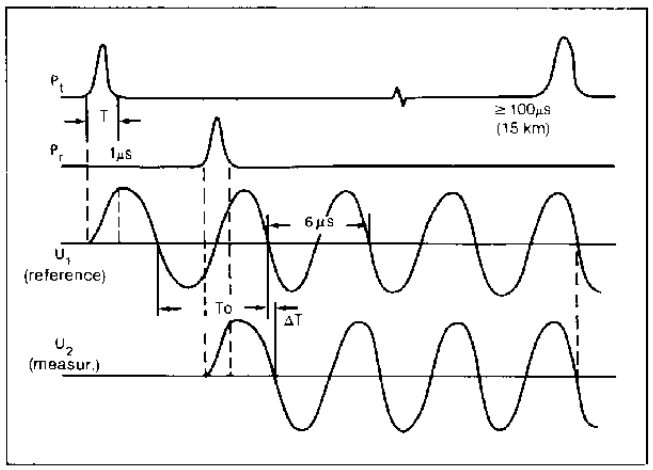

Fig. 14b

independent of the measurement approach, and is discussed in Section 5.

As we see from the block diagram in Fig. 13, a linear scanning frequency modulation from 53 to 67 MHz, generated in a surface acoustic wave device (SAW), is imposed at the output of the CO_2 laser, via an acoustooptic Ge/Li $Nb0_3$ [21] modulator for a duration of 4 μs. The electrical signal U, fed from the cadmium mercury telluride (CTM) detector, is then sent to another SAW which performs the pulse compression and reduces the pulse width by a factor of 40 (the theoretical compression ratio being 4 μs x 14 MHz = 56) i.e. to 100 ns (signal U'). This signal can thus be rectified and treated for the measurement of time intervals in the conventional way. The performance of the telemeter, to within a good approximation, is then equal to that of a normal pulse telemeter with $P_t = 3W \times 40 = 120$ W and $\tau = 100$ nsec. It may be noted that to prevent ambiguity of measurement it is necessary that the repetition time T be at least $2L_{max}/c$, and in [20] the choice has been made of T = 33 μs for L_{max} = 5 km.

The high repetition rate that results (30 kHz) allows the integration of many echo pulses with the known improvements in the probability of detection and of false alarm.

It is interesting to observe how, by average of successive measurements performed with chirps alternately increasing and decreasing in frequency, the radial velocity error is cancelled, while the time difference between the signals received with the two chirps allows the determination of the radial velocity of the target with a typical accuracy of 1 m/s.

In this instrumental approach, it appears interesting in the future to refine the choice of the transmitted waveform for the purpose of pulse compression with minimum sidelobes also in the presence of Doppler shifts [22-24], or of multiple echoes. However, the advantages of the technique of pulse compression, which in the microwave case are substantially linked to the low liability to interference due to the code structure of the signal employed, are not nowadays so important for the optical telemeter which is not yet significantly disturbed by electronic countermeasures.

Perhaps in the optic case it is more important the fact that this technique employs signals which are long in time, may usually be generated with good coherence and therefore are more suitable for heterodyne detection than the short pulses obtained with Q-switching techniques.

4.4 VERNIER TECHNIQUE FOR TELEMETRY WITH LONG PULSES

Another simple instrumental method of measurement which may be proposed with long pulse sources (in the microsecond region) is that of the vernier already adopted to increase time resolution in nuclear electronics [25]. Fig. 14a shows the implementation of the time vernier: the two measure and reference photodiodes feed the current pulses (see Fig. 14b) to two resonant circuits tuned at slightly different frequencies f_1 and f_2.

The frequency f_1 is chosen smaller than 1/T (e.g. 0.3 to 0.1/T) and f_2 is taken equal to $f_1(1 + 1/N)$ where N is the resolution of the measurement, i.e. the factor by which we desire to improve the minimum resolved interval of distance, with respect to that corresponding to the period of f_1 i.e. $L = c/2f_1$. For example, for f_1 = 150 kHz, L = 1 km and for N = 200 we resolve with the least significant digit L/N = 5m, by taking $f_2 = 150 \times 1.005$ kHz. Since for $f_1 \ll 1/T$ the zero crossings of the signals U_1, U_2 are seen to be strictly correlated with the centroid of the optical pulse [14-16], delayed by the periods $1/f_1$ and $1/f_2$ respectively, the coarse distance measurement (in units of $c/2f_1$ = 1 km) is obtained counting the number of periods contained in U_1 up to the first semiperiod of U_2 (time T_o in Fig. 14b) and the fine one is obtained counting the periods contained in U_1 after the first semiperiod of U_2 and until this signal does not anticipate U_1, counts which

provide the steps of $c/2f_1N = 5m$ in our case.

We note that the resonant circuits can be realised with quartzs or adequately accurate active filters, and that the detector with a resonant load is a good circuit solution to reduce the electronic noise associated with the termination of the preamplifier (contribution P_{eq})

On the basis of the data of Figs. 4 and 5, we may estimate the peak power adequate for a good telemetry in the near infra-red region as a few kilowatts. This power may be generated with a crystal source or with a GaAs injection laser diode array [26]. The weak point of the technique is the absence of immunity to retrodiffusion interference, as in the CW telemeters (Par. 4.2.).

5. Developments in optical detection

As we have seen, while for direct detection we do not reach a performance limited by the quantum noise at the maximum operational distances of a telemeter, the coherent detection gives us a heterodyne gain for the signal and relative fluctuations, but not for the background and electronic noise, thus allowing this quantum limit to be easily reached even at source powers lower than those used in a pulsed telemeter. More precisely, in the case of heterodyne detection with a local oscillator of power P_{OL} on the photodetector, the current at the output of the latter will be:

$$i_r = \frac{M \eta e}{h \nu} \sqrt{P_r P_{OL}} \qquad (37)$$

while the equivalent noise optical power at the input is:

$$P_n = \left[\frac{2 h \nu}{\eta} F(M) P_{OL} B \right]^{1/2} \qquad (38)$$

provided that $P_{OL} \gg P_r, P_b, P_v, P_{eq}$, a condition which can be easily satisfied. Under these conditions S/N is always at the optimum value given by (14) as may be immediately deduced. Gains in sensitivity, i.e. in reduction of the optical power necessary, from 10^2 to 10^3 have been quoted [20] [27] for heterodyne reception with CO_2 sources, while in the visible range, with the He-Ne sources used in interferometry [28], gains of 20-50 are commonly obtained without special care.

Obviously the requirement imposed by the heterodyne detection is the coherence between the received signal and the local oscillator beam, usually taken off as a part of the beam coming from the source. This must thus generate a longitudinal single mode emission to ensure spatial coherence, and possibly be stabilized in frequency to ensure the time coherence in the interval of flight time $2L_{max}/c$ (generally not greater that 100 μs). In fact, in this time the thermal drifts and environmental vibrations could induce a variation Δd of the length of the cavity d such as to generate a not negligible frequency error $(\Delta d/\lambda)\, c/d$.

The matching on the surface of the photodetector of the signal and reference wavefronts, necessary to maximize the beat signal (spatial coherence), is usually obtained by using a single optics for transmission and reception, and an optical interferometer type of configuration for the superposition of the beams.

Another alternative is that of using the source itself as the element of beam recombination, i.e. exploiting the same laser mirrors as selective element: if the longitudinal mode is splitted (through Zeeman effect, for example) in two oscillations of little different frequency, we can use one of them after the propagation to disturb the other. Thus we have the effects of induced modulation and injection modulation [9] [29], which allow a supplementary internal gain with respect to the conventional heterodyne detection.

Finally the degradation of the coherence due to the propagation should be taken into account. Since, in general, beams of dimensions greater than the microscale of the turbulence are transmitted, there is in effect a loss of spatial coherence in the propagation of the beam. Further, the time fluctuations of the turbulence induce a variation in the frequency of the received waveform.

The loss of coherence may be presented schematically as being equivalently due to a random vibration of the target being measured (time effects), combined with the purely random distribution of the diffusion characteristics of its surfaces (spatial effects). Under these conditions, the returned field is of a time-variable speckle-pattern type. If, nevertheless, we put the receiver within the diffraction angle associated with the target dimensions, the received field is still spatially coherent, even if it contains a random phase term and has an amplitude with an exponential probability distribution [30,31].

Therefore it is possible to carry out a coherent detection of the signal provided that we take into account that the amplitude is variable and is subject at certain points to fading, and that the phase fluctuations produce a widening of the bandwidth of the signal itself.

REFERENCES

[1] *J.C. Owens* "**Laser Applications in Metrology and Geodesy**" in: Laser Applications, vol. I, ed. by M. Ross, Academic Press, New York, 1971.

[2] *M. Françon* "**Optical Interferometry**" Academic Press, New York, 1966.

[3] *R. Baldwin, G. Gordon, A. Rudè* "**Remote Laser Interferometry with 5525 HP**" Applic. Note 156-1, Hewlett Packard, Palo Alto, 1972.

[4] *D.E. Smith* "**Distance Measurement for Industrial and Scientific Applications**" Hewlett Packard Journal, June 1980.

[5] *K.D. Froome* "**Distance Measurement by Means of Modulated Light**" Alta Frequenza *41* (1972), p. 753-758.

[6] *R.H. Bradsell* "**Telemetry with Modulated Beams, Short Range Systems**" Alta Frequenza *41* (1972), p. 759-770.

[7] *C.M. Johnson* "**Laser Radars**", in Radar Handbook, ed. M.I. Skolnik" MacGraw-Hill Book Co., New York, 1970.

[8] *C.G. Bachman* "**Laser Radar Systems and Techniques**" Artech House Inc., Dedham, Mass., 1979.

[9] *S. Donati* "**Laser Interferometry by Induced Modulation**" J. Appl. Phys. *49* (1978), p. 495-498.

[10] *RCA* "**Electro-Optics Handbook**" RCA, Harrison, 1974.

[11] *W. Eppers* "**Atmosphere Transmission**", in CRC Laser Handbook, Chemical Rubber Co., 1970.

[12] *A.P. Thomas, M.P. Thekaekara* Proc. Joint Conf. Am. Sect. ISES and SES, Aug. 1976, p. 338-340.

[13] *M.I. Skolnik* "**Introduction to Radar Systems**" McGraw-Hill Book Co., New York, 1962.

[14] *E. Gatti, V. Svelto* "**Optimum Filter for Timing**" Nucl. Instr. and Methods *39* (1966), p. 309-313.

[15] *E. Gatti, C. Cottini, S. Donati, V. Svelto* "**Pulse Shape Discrimination**" Energia Nucleare *17* (1970), p. 34-45.

[16] *S. Donati, E. Gatti* "**Beam Modulation Telemetry**" in Laser Applications, ed. by A. Sona, Gordon & Breach, New York, 1975.

[17] *E. Gatti, S. Donati* "**Optimum Signal Processing for Laser Telemetry**" Appl. Optics *10* (1971), p. 2446-2451.

[18] *E. Angeleri* "**Trasmissione Dati**" Delfino, Milano 1972.

[19] *C.J. Oliver* "**Pulse Compression in Optical Radar**" IEEE Trans. *AES-15* (1979), p. 306-324.

[20] *K.F. Hulme, B.S. Collins, G.D. Constant, J.T. Pinson;* "**A CO_2 Rangefinder using Heterodyne Detection and Chirp Pulse Compression**" Opt. and Quant. Electron. *13* (1981), p. 35-45.

[21] *B.S. Collins, K.F. Hulme, N.A. Lowde* "**Acusto-Optic Modulator for a CO_2 Laser Rangefinder**" Opt. and Quant. Electron. *12* (1980), p. 419-426.

[22] *G. Galati, V. Linardi, V. Marziali* "**Valutazione e Confronto di Forme d'Onda per Applicazioni Radar**" Alta Frequenza *47* (1978), p. 484-494.

[23] *G. Galati, V. Linardi, V. Marziali* "**Sintesi di Forme d'Onda per Applicazioni Radar**" Alta Frequenza *47* (1978), p. 65-77.

[24] *T. Bucciarelli, G. Picardi* "**Eliminazione dei Lobi Laterali in Ricevitore Adattato a Codici Barker**" Alta Frequenza *47* (1978), p. 728-734.

[25] *K. Kowalski* "**Nuclear Electronics**" J. Wiley, Chichester, 1975.

[26] *S. Donati* "**Strumento per la Visione Attiva a Bassi Livelli di Illuminamento**" Riunione AEI, Roma, 1974, Memoria B13.

[27] *J.M. Cruickshank* "**TEA CO_2 Laser Radar with Heterodyne Detection**" Appl. Opt. *18* (1979), p. 290-293.

[28] *S. Donati* "**A Novel Laser Interferometer for Distance Measurements**" Conf. on Precision Electromagn. Measur., Ottawa, 1978, Digest p. 76-77.

[29] *V. Annovazzi Lodi, S. Donati* "**Injection Modulation in Coupled Laser Oscillators**" J. Quant. El. *QE-16* (1980), p. 859-864.

[30] *W. Goodman* "**Statistical Properties of the Speckle Pattern**" Cap. II, Topics in Appl. Phys. Vol. *9*, ed. by Dainty, Springer Verlag, Berlin, 1977, p. 9-75.

[31] *S. Donati, G. Martini* "**Speckle Pattern Intensity and Phase: Second Order Conditional Statistics**", J. of the Opt. Soc. of America *69* (1979), p. 1690-1694.